Intramolecular Electron Transfer between [4Fe-4S] Clusters Studied by Proton Magnetic Resonance Spectroscopy

Panayotis Kyritsis,[‡] J. Gaspard Huber,[§] Isabelle Quinkal,[‡] Jacques Gaillard,[§] and Jean-Marc Moulis*,[‡]

Département de Biologie Moléculaire et Structurale, Laboratoire Métalloprotéines, et Département de Recherche Fondamentale sur la Matière Condensée, SCIB-SCPM, CEA/Grenoble, 17 rue des Martyrs, 38054 Grenoble Cedex 9, France

Received January 3, 1997; Revised Manuscript Received April 7, 1997[⊗]

ABSTRACT: The rate constants for the intramolecular electron transfer between the two [4Fe-4S] clusters of a series of native and genetically engineered ferredoxins have been determined by proton magnetic resonance (^{1}H NMR) spectroscopy. The measurement relies on the properties of the signals assigned to β-protons of the coordinating cysteines when the protein is substoichiometrically reduced: these signals include coalesced peaks arising from the fast hopping of an extra electron between the two oxidized clusters of the protein. An upper limit of significantly less than 10^5 M^{-1} s^{-1} for the intermolecular and an average of the order of 5×10^6 s^{-1} for the intramolecular electron transfer rate constants of several ferredoxins have been obtained. Owing to the edge-to-edge intercluster distance of approximately 10 Å derived from the crystallographic structure of *Clostridium acidurici* ferredoxin, the rate constant associated with the intramolecular process is as expected for a nonadiabatic redox process, assuming a reasonable value of less than 1 eV for the reorganization energy. The latter could not be determined from the temperature dependence of the rate constant since no variation was observed over the temperature range accessible in these experiments. Structural changes introduced around and between the two [4Fe-4S] clusters in *Clostridium pasteurianum* ferredoxin by site-directed mutagenesis have been used to probe the potential involvement of dominant electron transfer pathways between the clusters. These changes have no major effect on the value of the intramolecular electron transfer rate constant. From this analysis, no specific amino acid side chain seems to play a central role in the process. The rate constants derived in the present work may serve as a basis for the study of enzymes containing two closely spaced [4Fe-4S] clusters such as found in these ferredoxins.

The transfer of electrons is one of the most important chemical steps in biological reactions. Long-range (i.e., beyond 5 Å) electron transfer (ET)[1] sustains basic biological functions, such as photosynthesis, respiration, and nitrogen fixation (Lippard & Berg, 1994). These processes result in a net vectorial flow of electrons over considerably long distances in the protein matrix, across the ca. 40 Å membrane separating lumen from stroma in the case of photosystem I, for example (Chitnis, 1996; Brettel, 1997). Biological systems cope with the problem of moving charges through the protein matrix by regularly spacing various redox cofactors—e.g., metal atoms or organic moieties—every 5−25 Å along the way. Such design ensures efficient and highly specific flow of electrons as required in each case. Despite the diversity of systems obeying this schematic arrangement and the number of studies dealing with biological ET systems, the factors that control speed and specificity at the molecular level are still largely unknown. One of the most recent examples is provided by cytochrome *c* oxidase, in which ET from Cu_A to either hemes *a* or a_3 proceeds at very different apparent rates (Winkler et al., 1995; Einarsdóttir, 1995), despite the similar distances separating these redox centers, ca. 21 and 23 Å, respectively (Tsukihara et al., 1996).

A lot of experimental work has been devoted to large and integrated biological ET systems such as cytochrome *c* oxidase (Capaldi, 1996) or photosystems (Nugent, 1996), including extensive studies on the reaction centers (Moser et al., 1995). Despite the complexity and relative lack of precision associated with the structures of these big molecules, the conclusions drawn from studies on the reaction centers have led to a general model of biological ET (Moser et al., 1995). A different approach, namely, the use of smaller ET molecules such as cytochromes, Cu proteins, or flavoproteins, has proved complementary and is providing evidence that in some cases ET depends on the structural features of the redox protein (Karpishin et al., 1994). For the most part, these studies rely on the possibility of engineering an artificial redox center into these molecules besides the native cofactor and to study intramolecular ET inside these well-characterized molecules (Gray & Winkler, 1996). A more recent approach aims at designing and synthesizing ET proteins with specific structural properties, the so-called ET maquettes (Robertson et al., 1994). A common feature of all these studies is to obtain two redox centers in a well-characterized protein framework.

These requirements are found in only a few natural systems. Among these, ferredoxins (Fd) containing two [4Fe-4S] clusters are particularly suitable proteins to study. Indeed, the X-ray structures for the proteins from *Pep-*

* Address correspondence to this author at DBMS/MEP, CEA/Grenoble, 17 rue des Martyrs, 38054 Grenoble Cedex 9, France. Telephone 33 (0)476885623; Fax 33 (0)476885872; e-mail moulis@ebron.ceng.cea.fr.

‡ Département de Biologie Moléculaire et Structurale.

§ Département de Recherche Fondamentale sur la Matière Condensée.

⊗ Abstract published in *Advance ACS Abstracts,* June 1, 1997.

[1] Abbreviations: ET, electron transfer; Fd, ferredoxin; EPR, electron paramagnetic resonance; NMR, nuclear magnetic resonance; EXSY, exchange spectroscopy.

S0006-2960(97)00020-2 CCC: $14.00

tostreptococcus asaccharolyticus (Adman et al., 1976), *Clostridium acidurici* (Duée et al., 1994), and *Chromatium vinosum* (Moulis et al., 1996) have been solved. Despite the very similar structure around the two clusters (Moulis et al., 1996) in all these simple (less than 100 amino acids) proteins, very significant changes in the efficiency of ET between the two clusters have been observed (Huber et al., 1995). This family of proteins thus constitutes a valid model to address the above-mentioned question of the factors controlling ET rates. In addition to their thorough structural characterization, they have been found to be amenable to extensive genetic engineering (Davasse et al., 1995) and to a variety of spectroscopic investigations (Johnson, 1994).

However, quantitative kinetic studies have been up to now restricted to the intermolecular ET properties of these molecules with various redox partners (Armstrong, 1982; Navarro et al., 1989; Quinkal et al., 1996) because the two [4Fe-4S] clusters, which lie at a center to center distance of ca. 12 Å, cannot be easily distinguished spectroscopically. The method of choice to solve this problem is ^{1}H NMR spectroscopy: the very slight structural differences around the two clusters induce slightly different chemical shifts of the surrounding protons, particularly those of the coordinating cysteines (Packer et al., 1977; Bertini et al., 1992, 1994; Gaillard et al., 1993). This property has been used to estimate a lower limit for the intramolecular ET rate constant in half-reduced (one cluster oxidized, the other reduced in the same molecule) samples (Bertini et al., 1992).

In the present work, quantitative kinetic data have been derived for these reactions and possible effects of structural changes around and between the two clusters have been addressed using molecular variants of *Clostridium pasteurianum* Fd. The intramolecular electron exchange could be physiologically relevant by establishing a vectorial flow of electrons between the redox partners of ET chains *via* the two [4Fe-4S] clusters of Fd (Quinkal et al., 1994; Moulis & Davasse, 1995). In addition, this arrangement of two closely spaced [4Fe-4S] clusters occurs in a wide range of more complex ET systems, such as photosystem I (Chitnis, 1996), NADH−ubiquinone oxidoreductase of the mitochondrial respiratory chain (Walker, 1992), and various other enzymes, such as *Escherichia coli* dimethyl sulfoxide reductase subunit DmsB or *C. pasteurianum* hydrogenase [Quinkal et al. (1994) and references therein]. Of particular importance is the comparison with the two [4Fe-4S] centers, denoted as F_A and F_B, which act as terminal membrane-bound electron acceptors of photosystem I. They are held by subunit PsaC, a peptide homologous to bacterial 2[4Fe-4S] Fds, and they have been shown by X-ray crystallography to be at a similar intercluster distance of ca. 12 Å (Krauss et al., 1996).

EXPERIMENTAL PROCEDURES

Preparation of Proteins. Recombinant *C. pasteurianum* 2[4Fe-4S] Fd was produced in *E. coli* from a synthetic gene, as previously described (Davasse & Moulis, 1992; Moulis et al., 1994). Site-directed mutagenesis by oligonucleotide modular replacement was used to obtain molecular variants (Gaillard et al., 1993; Quinkal et al., 1994). *C. acidurici* Fd was isolated as previously described (Gaillard et al., 1986).

NMR Spectroscopy. The preparation of Fd for NMR experiments has already been presented (Gaillard et al., 1993). For measurements of intramolecular ET rate constants, protein samples (0.5−2.2 mM) were in 20 mM potassium phosphate buffer, pH 8.2, containing 10% D_2O.

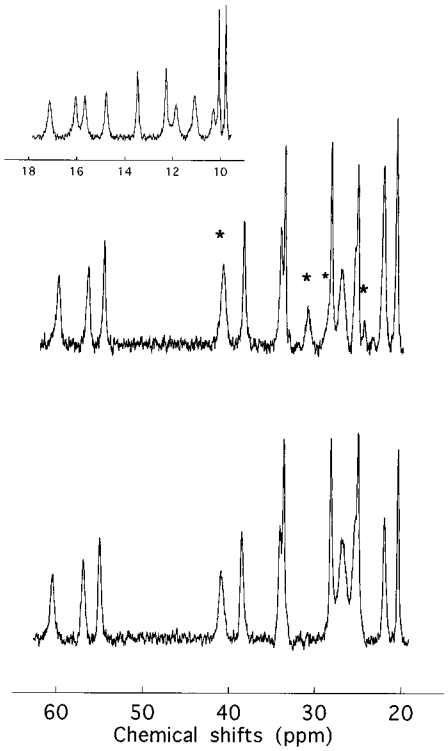

FIGURE 1: Low-field part of the ^{1}H NMR spectra of *C. pasteurianum* ferredoxin: upper spectrum, fully oxidized protein; middle spectrum, semireduced; lower spectrum, fully reduced. The positions of some of the intermediate peaks are starred.

^{1}H NMR experiments were carried out at 298 K, unless stated otherwise, on a Varian 500 MHz Unity Plus spectrometer as previously described (Huber et al., 1995). The values of the transverse relaxation times T_2 were determined from the line widths and an average precision of 10% on these values was estimated, although larger errors may be associated with some shifted resonances in the spectra of the reduced or semireduced proteins.

Other Methods. The thermal stability of 2[4Fe-4S] Fd was estimated as in previous work (Quinkal et al., 1994). The search for favorable ET pathways between the clusters of 2[4Fe-4S] Fd has been carried out using the highest resolution structural model published for *C. acidurici* Fd (Duée et al., 1994) with the program Greenpath v0.97 (Regan et al., 1995) implementing the electronic coupling dependencies previously estimated (Regan et al., 1993).

RESULTS

Evidence for ET Reactions in ^{1}H NMR Spectra. The ^{1}H NMR spectra of oxidized, $2[4Fe\text{-}4S]^{2+}$, and reduced, $2[4Fe\text{-}4S]^{+}$, *C. pasteurianum* Fd have already been reported (Phillips & Poe, 1973; Gaillard et al., 1987, 1993; Bertini et al., 1990, 1992). When the oxidized protein is reduced by less than two electrons, the spectrum is not the mere superimposition of the spectra of the oxidized and reduced protein (Figure 1). The resonances of the fully reduced and fully oxidized species are complemented by additional signals that appear at intermediate chemical shifts between those of the signals of the oxidized and reduced protein. The most shifted signals of Figure 1 were assigned to the β-protons of the coordinating cysteines (Packer et al., 1977; Bertini et

al., 1992), which—owing to the magnetic moment of the $[4Fe\text{-}4S]^{1+/2+}$ clusters—are shifted outside the diamagnetic envelope and well resolved. Cross-correlations between peaks for the oxidized, reduced, and half-reduced species at an intermediate redox level of the protein by EXSY experiments (Bertini et al., 1994) extended the complete assignments of the β-protons of the coordinating cysteines of the oxidized protein to the other redox levels. These observations indicate that the spectroscopic features specific to the intermediate redox level can be interpreted as due to fast—compared to the resonance frequency difference of the signals for the fully reduced and oxidized species—electron exchange between the clusters. The spectra of semireduced 2[4Fe-4S] Fd are thus the combination of the intrinsic spectra of the protein at two different redox levels (oxidized and reduced) with kinetic redox processes potentially involving both inter- and intraprotein ET.

Intermolecular Electron Exchange. The occurrence of chemical exchange, such as the ET reactions described above, influences both the chemical shifts and relaxation times of the NMR signals (Sandström, 1982). The different NMR regimes observed in electron-transfer proteins and the information derived in each case have been recently summarized (Gaillard et al., 1996). In the case of the intermediate redox level in Figure 1 the resonances already observed in the spectra of the fully reduced or fully oxidized *C. pasteurianum* Fd correspond to subpopulations of the mixture that contain either two reduced or two oxidized clusters. These species take part in intermolecular ET with other components of the mixture as evidenced by EXSY experiments, a process that may broaden the corresponding peaks. However, neither broadening nor chemical shift effects have been observed as a function of the concentrations of these subpopulations within the limits of the accuracy of the peak-width measurements. Therefore, the rates of (intermolecular) electron exchange involving these species are not kinetically significant when compared to the transverse relaxation rates of the oxidized or reduced signals observed in Figure 1. The large chemical shift separation between correlated peaks of different redox levels translates into second-order rate constants smaller than 10^5 M^{-1} s^{-1}. This value decreases by almost one order of magnitude if the precision of the NMR line widths is supposed to hinder the observation of the broadening effect.

Intramolecular Electron Transfer. When the resonance frequency difference between the signals of the same proton in two redox environments—fully reduced and fully oxidized—is smaller than the rate of electron exchange, the two signals are coalesced as observed in Figure 1. The positions and line widths of these coalesced peaks depend neither on the concentration of protein nor on that of the subpopulation of molecules containing one cluster reduced and one oxidized, as observed, for example, during the redox titration of the protein. Therefore, the existence of these intermediate resonances reflects the intramolecular ET occurring between the two clusters without significant contribution from intermolecular processes.

The chemical shifts (δ_{int}) and the transverse relaxation times (T_{2int}) of these relatively broad coalesced peaks are given by the following equations (Gaillard et al., 1996):

$$\delta_{int} = f_{ox}\delta_{ox} + f_{red}\delta_{red} \quad (1)$$

$$1/T_{2int} = f_{ox}/T_{2ox} + f_{red}/T_{2red} + f_{ox}f_{red}k^{-1}[2\pi(\nu_{ox} - \nu_{red})]^2 \quad (2)$$

where f_{ox} is the fraction of time the cysteinyl proton is in the oxidized environment (i.e., cluster coordinated by this cysteine oxidized in 2[4Fe-4S] Fd), f_{red} is the fraction of time that the proton is in a reduced environment (adjacent cluster reduced), k is the first-order rate constant for intramolecular electron exchange, and $T_{2ox/red}$ are the transverse relaxation times and $\nu_{ox/red}$ the resonance frequencies of the signal in the oxidized and reduced environments without exchange. It follows from eq 1 and from the fact that for a given proton $f_{ox} + f_{red} = 1$ that

$$f_{ox} = (\delta_{red} - \delta_{int})/(\delta_{red} - \delta_{ox}) \quad (3)$$

In eqs 1 and 2 the chemical shift and transverse relaxation time of the intermediate signal resulting from fast exchange depend on the corresponding parameters of the signals for the oxidized and reduced states. The relevant $\delta_{ox(red)}$ and $T_{2ox(red)}$ in these equations should be associated with states in which one cluster is oxidized and the other reduced *in the absence* of exchange. Such conditions cannot be generated and these parameters cannot be measured. No direct evidence for changes in the chemical shifts or relaxation times of a signal belonging to one ligand of one cluster as a function of the redox level of the other cluster of the same molecule is available for the ferredoxins studied herein, although some experimental results (Benelli et al., 1994) might be interpreted by implicating such changes. We have assumed here that $\delta_{ox(red)}$ and $T_{2ox(red)}$ are the same as the ones for the *exclusively* oxidized or reduced species. In other words, the oxidation state of the second cluster is supposed not to affect the chemical shifts and the relaxation times of the signals of protons surrounding the first. Results on the temperature dependence of f_{ox} and f_{red} presented herein appear to sustain this assumption, at least for chemical shifts (see below).

In line with previous publications, we label the cluster coordinated by Cys-8, Cys-11, Cys-14, and Cys-47 as cluster I and the one coordinated by Cys-37, Cys-40, Cys-43, and Cys-18 as cluster II (Figure 2). Equation 2 implies that the most accurate values for k will be obtained from signals whose difference in chemical shifts between fully reduced and fully oxidized proteins is maximum and for which the intermediate peak is well resolved.

In *C. pasteurianum* Fd the protons that meet both these criteria are Hβ_2C40, Hβ_1C43, and Hβ_2C47. In the case of Hβ_2C40 the difference ($\Delta\delta = \delta_{red} - \delta_{ox}$) may not be as large (21.6 ppm at 298 K) as for other peaks but the intermediate peak Hβ_2C40$_{int}$ is well resolved. In contrast, $\Delta\delta$ is larger for Hβ_2C47 and Hβ_1C43 (>40 ppm) but Hβ_2C47$_{int}$ and Hβ_1-C43$_{int}$ overlap with other signals over part of the temperature range. The most suitable protons in the case of other proteins have been determined accordingly. The relevant parameters concerning these protons along with the calculated rate constants k are listed in Table 1. Similar rate constants have been measured in buffer prepared with 90% H_2O or 90% D_2O.

The intramolecular electron-transfer rate constant of *C. pasteurianum* Fd has been determined over the 283−308 K temperature range accessible in these experiments and has not been found to vary (Figure 3). Indeed, if the errors

Table 1: Intramolecular Electron Transfer Rate Constants and Reduction Potential Differences between the Two Clusters of Ferredoxins[a]

	Cp Fd	*Ca* Fd	I23V	V20R	P19K	F30I
δ_{ox} (ppm)	13.25	13.7	16.52	16.01	16.1	13.7
δ_{int} (ppm)	28.91	32.57	39.20	46.11	38.4	34.3
δ_{red} (ppm)	56.72	56.24	62.19	57.50	59.9	63.9
f_{ox} (%)	64	56	50	27	50	59
f_{red} (%)	36	44	50	73	50	41
$1/T2_{ox}$ (Hz)	134	271	221	224	223	144
$1/T2_{int}$ (Hz)	1005	972	1413	1680	1306	1941
$1/T2_{red}$ (Hz)	556	314	650	1290	757	672
k_{intra} ($\times 10^{-6}$ s^{-1})	6 ± 1.3	6.5 ± 1.3	5.3 ± 1	4.9 ± 2	5.8 ± 1.5	4.0 ± 1.5
$\Delta E°$ (mV)	15	6	0	26	0	10

[a] These data were obtained for $H_{\beta 2}$C47 in the cases of the native ferredoxins from *C. pasteurianum* (*Cp*) and *C. acidurici* (*Ca*) and of the F30I variant of *Cp*Fd. In the cases of the other variants of *Cp*Fd, $H_{\beta 1}$C43 was used instead. Therefore, f_{ox} refers to the fraction of time cluster I is oxidized in the former cases and to the fraction of time it is reduced in the latter.

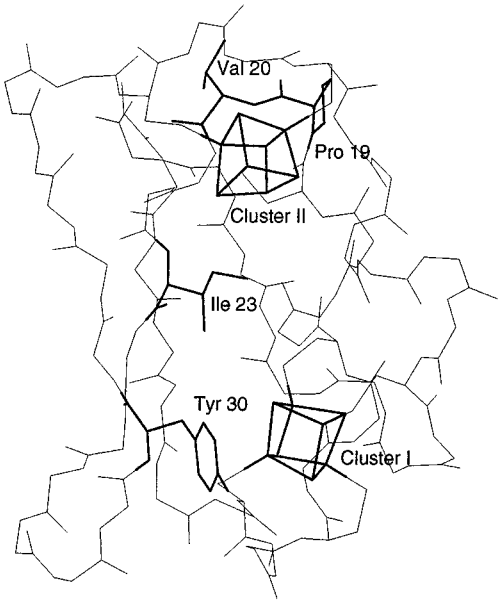

FIGURE 2: Folding of *C. acidurici* ferredoxin. The two [4Fe-4S] clusters and the residues of *C. pasteurianum* ferredoxin substituted in this work are highlighted.

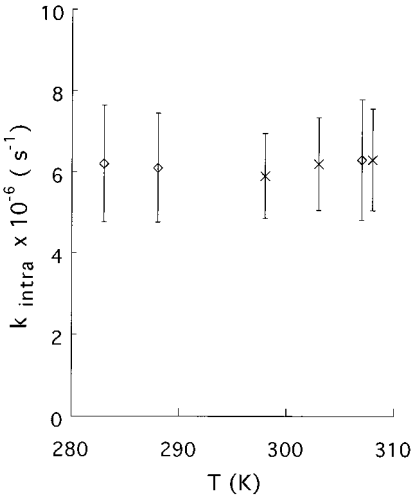

FIGURE 3: Variation of the intramolecular ET rate constant for *C. pasteurianum* ferredoxin with temperature. The values were calculated for the $H_{\beta 2}$C47 (crosses) and $H_{\beta 1}$C43 (diamonds) protons. The error bars are estimated as described under Experimental Procedures.

associated with the measurements are taken into account, an upper limit, and most probably a significantly overestimated one, of 1.5-fold increase can be evaluated between 283 and 308 K. The results shown in Figure 3 suggest that it is more realistic to consider *k* as temperature-independent.

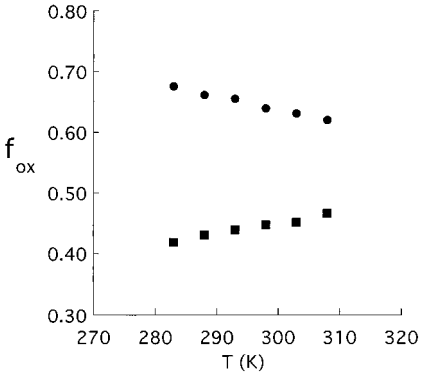

FIGURE 4: Variation of the parameter f_{ox} for *C. pasteurianum* ferredoxin with temperature. Squares, data from the $H_{\beta 2}$C40 proton (cluster II); circles, data from the $H_{\beta 2}$C47 proton (cluster I).

Parameters f: Estimation of Reduction Potential Differences. The chemical shifts of the β-protons of the coordinating cysteines in *C. pasteurianum* Fd for the fully reduced, fully oxidized, and semireduced levels give f_{ox} by eq 3 (Table 1). This is a measure of the difference ($\Delta E°$) of the reduction potentials between the two clusters, and the driving force ($\Delta G°$) associated with the intramolecular electron exchange can be estimated (Table 1). Of particular note is the fact that the f_{ox} values get nearer to 0.5 when the temperature is increased (Figure 4). The intermediate peaks would then occur approximately midway between the resonances of the same proton in the fully oxidized and fully reduced protein at high temperature. This observation suggests that the chemical shifts of eq 3 used in the calculations are reasonable and supports the assumption made above for *C. pasteurianum* Fd about the actual values of $\delta_{ox(red)}$ in eq 2 for the calculations of *k* (Table 1).

Intramolecular ET Rate Constants in Related Proteins. Since a relatively accurate estimate of the intramolecular ET rate constant in 2[4Fe-4S] Fd could be obtained, it was of interest to investigate whether structural changes introduced around the clusters would affect these values. First, the homologous Fd from *C. acidurici* gave a value similar to that determined for *C. pasteurianum* Fd (Table 1). These two proteins share a series of aliphatic residues surrounding the clusters and contributing strongly to shield the active sites from the solvent (Adman et al., 1976; Duée et al., 1994). Among them, I23 lies between the clusters and its interactions with them have been suggested as important in the intramolecular communications (Duée et al., 1994). V20 and P19 participate in building the hydrophobic environment for

Table 2: Kinetic Constants for Thermal Denaturation of *C. pasteurianum* Fd I23 Variants[a]

	native Fd	I23L	I23V
k (% h^{-1})	1.8	4.8	3.6

[a] These values were determined at 55 °C under anaerobic conditions as previously described (Quinkal et al., 1994).

Table 3: Chemical Shift Differences for Selected Cysteinyl Protons Induced by Site-Directed Mutagenesis[a]

proton	δ native	$\Delta\delta$ P19K	$\Delta\delta$ F30I	$\Delta\delta$ V20R	$\Delta\delta$ I23V
H$_{\beta1}$C43	60.51		−5.4	−3.3	
H$_{\beta2}$C47	56.87		+7.13		
H$_{\beta2}$C8	55.00				
H$_{\beta1}$C8	40.96		+4.5		
H$_{\beta2}$C40	38.48	+7.0			
H$_{\beta2}$C11	34.07		+5.4		
H$_{\beta1}$C40	33.61	+9.2			
H$_{\beta2}$C37	28.26	−3.4			+3.8
H$_{\beta1}$C47	26.90				
H$_{\beta2}$C18	24.98	+5.9		+10	
H$_{\beta1}$C14	25.47				

[a] Chemical shifts in parts per million were measured at 295 K for fully reduced proteins. For molecular variants of *C. pasteurianum* ferredoxin, only chemical shift differences (mutated form−native) larger than 3 ppm are reported. Assignments were initially proposed by Bertini et al. (1994).

cluster II, as Y30 (F in *C. pasteurianum* Fd) does for cluster I (Carter, 1977). All these residues (Figure 2) may be important for the function of the protein, as already probed for some of them (Quinkal et al., 1994).

A series of plasmids in which the codon for I23 was replaced by those for P, G, A, V, L, E, Q, R, F, M, T, or S have been generated. Among them, only those encoding the I23L and I23V forms produce recombinant proteins. The I23L and I23V variants contain the two [4Fe-4S] clusters but are less stable than the native form (Table 2). The above observations indicate that the hydrophobic side chain of I23 has an important stabilizing role for the protein. However, the structural changes witnessed by the decreased stability of I23V do not translate into a significantly different intramolecular ET rate constant (Table 1).

In contrast to I23, V20 is a position in *C. pasteurianum* Fd that can be substituted by G, A, H, or R. Only the variant V20P displaying two successive proline residues could not be purified. Although small chemical shift differences for the cysteinyl signals assigned to Hβ_2C43 and Hβ_2C18 were detected in the NMR spectra of V20R (Table 3), the intramolecular ET rate constant did not significantly change from that of the native form (Table 1). Similarly, the previously obtained P19K (Gaillard et al., 1993) and F30L (Quinkal et al., 1996) variants displayed rate constants in the same range (Table 1).

DISCUSSION

Structural Variations among Molecular Variants. The present ^{1}H NMR study of 2[4Fe-4S] ferredoxins has given access to quantitative kinetic data for the ET process occurring between the two clusters. It confirms the lower limit of 10^5 s^{-1} estimated previously for *C. pasteurianum* Fd (Bertini et al., 1992). It is noteworthy that the slight structural changes introduced by site-directed mutagenesis of *C. pasteurianum* Fd or by use of another natural protein (Table 1) do not drastically modify this value. The fact that indeed structural changes are introduced in these molecular variants is borne out by the clear detection of differences in chemical shifts for the ^{1}H NMR signals associated with the cysteinyl Hβ of the ligands (Table 3). These values are good reporters of the detailed geometry of the ligands and of the electronic distribution on the clusters (Mouesca et al., 1993; Bertini et al., 1994; Huber et al., 1995), and the origin and nature of the structural changes have been established in detail for P19K (Quinkal et al., 1994).

In the case of the I23-substituted *C. pasteurianum* Fd variants, additional large destabilizing effects result from removal of the hydrophobic terminal δ-methyl of isoleucine and neither polar, charged, nor bulkier side chains could replace that of isoleucine. These observations strongly indicate that I23 is one of the main contributors to the hydrophobic effect stabilizing this kind of protein. Moreover, although I23V (and I23L) could efficiently be produced, I23A could not. Considering the structure of 2[4Fe-4S] Fd around I23 (Duée et al., 1994), this is an example of cavity-creating changes introduced by site-directed mutagenesis. Such experiments have been carried out with several proteins [Fersht and Serrano (1993) and references therein] and led to the consensus that each methylenic group of aliphatic side chains contributes an average of 1.3 kcal/mol in conformational stability through the hydrophobic effect (Kellis et al., 1988; Eriksson et al., 1992; Pace, 1992). In the case of *C. pasteurianum* Fd, the inability to produce recombinant I23A correlates with its complete destabilization (Moulis et al., 1994) and gives an estimate of about 4 kcal/mol for the free energy difference between the folded and unfolded conformations of *C. pasteurianum* Fd. Although this value is a very rough estimate, it confirms the very poor stability of 2[4Fe-4S] Fd of the kind discussed herein when compared to most other studied proteins, even of similar sizes, which display conformational stabilities well above 5 kcal/mol.

Comparison between Measured and Predicted ET Rate Constants. Considering that ET reactions in proteins result from electron tunneling and nuclear rearrangements (Marcus & Sutin, 1985), the rate constant for a nonadiabatic process is given by

$$k = 2\pi/\hbar V_R^2 (4\pi K_B \lambda T)^{-1/2} \exp[-(-\Delta G^\circ - \lambda)^2/4K_B\lambda T] \quad (4)$$

In this equation ΔG° is the driving force, λ is the reorganization energy, and V_R is the electronic coupling. h ($=2\pi\hbar$) and K_B are the Planck and Boltzmann constants, respectively. The reorganization energy is a measure of the structural rearrangements occurring when the redox system changes its oxidation state. In the case of a redox metalloprotein there are contributions from the redox cofactors (inner reorganization energy λ_i) and the rest of the protein molecule, including the solvent (outer reorganization energy λ_o).

(i) Homogeneous Mediation of Electron Transfer. On the basis of the observation that the optimal (i.e., $-\Delta G^\circ = \lambda$) ET rate constants measured in many redox systems vary exponentially with the distance R separating the redox cofactors (Moser et al., 1992), the electronic coupling decay has been proposed not to depend on the structural features of the intervening protein medium: a linear dependence $V_R^2 = V_0^2 \exp[-\beta(R - R_0)]$ has been obtained, where V_0^2 is the

electronic coupling at van der Waals contact (R_0) and $\beta = 1.4$ Å^{-1} is the distance decay coefficient of V_R^2. Equation 4 was thus simplified for room-temperature rates to

$$\log k = 15.2 - 0.61R - 3.1(-\Delta G^\circ - \lambda)^2/\lambda \qquad (5)$$

where $(-\Delta G^\circ - \lambda)^2/\lambda$ is expressed in electron volts and distance R in angstroms (Moser et al., 1995).

The driving force for the intramolecular electron exchange in 2[4Fe-4S] Fd is very small and does not correlate with the measured rate constants (Table 1, Figures 3 and 4). Thus, a value $\Delta G^\circ = 0$ has been assumed in the following.

The reorganization energy λ is very difficult to determine experimentally since the most satisfactory experimental method is to construct plots of rate k against ΔG° and obtain λ at the maximum of the parabolic curve (eq 4). Studies of this type have only been performed for a few systems and an upper limit of 1.3 eV for λ in redox proteins has been deduced (Moser et al., 1992; Gray & Winkler, 1996). A range of values between 0.5 and 1.0 eV has been considered here: using the average of the *shortest* distances between the Fe atoms of the two [4Fe-4S] clusters (10 Å), eq 5 gives a range of theoretical rate constants between 1.0×10^6 and 3.5×10^7 s^{-1}, in good agreement with the experimental values listed in Table 1.

(ii) Dominant ET Pathways. Some experimental evidence in other systems does not obey the simplified relationship, eq 5, and has led to the proposal that there might be specific electron transfer pathways that dominate the electronic coupling between redox sites (Gray & Winkler, 1996). Accordingly, physicochemical considerations about the donor−acceptor interaction have assisted the building of numerical algorithms designed to determine favorable ET pathways through the structural details of the intervening medium (Onuchic et al., 1992; Regan et al., 1993).

In the present case of 2[4Fe-4S] Fd we have carried out this type of analysis on the 1.84 Å resolution model available for *C. acidurici* Fd (Duée et al., 1994). If the two equivalent, exclusively through-bond, pathways encompassing two cysteine side chains and the main chain of either of the 14−18 or 43−47 segments that link the two clusters are taken as references (Figure 5), a few pathways including through-space "jumps" are predicted to be more efficient. Among these pathways, the best ones evidently contain only one jump. The single through-space connection may occur between the Hβ_2 of cysteines 14 and 43, between Cys14O and Cys18HN (a predicted H-bond), or between Cys43O and Cys47Hβ_2. If two jumps are considered, they occur between Cys14Hβ_2 and Ile23HCδ and between the latter proton and Cys18Hβ_2 in the most efficient predicted pathway involving a side-chain atom other than one belonging to a cysteine (Figure 5).

The immediate conclusion from these calculations is that the electronic coupling between the two clusters is largely independent of the nature of the residues building the protein. Only when two energetically costly through-space interactions are considered may a side chain (Ile23) be important in the reaction. However, such a possibility cannot be completely dismissed on theoretical grounds. Isoleucine 23 is one of the most conserved residues among the family of clostridial 2[4Fe-4S] Fd and has been proposed to influence the interactions between the clusters (Duée et al., 1994). The removal of the δ methyl group of this residue clearly does not change the ET rate constant between the clusters (Table 1) and indicates that electronic coupling directly involving side-chain atoms is unlikely to be important in these proteins.

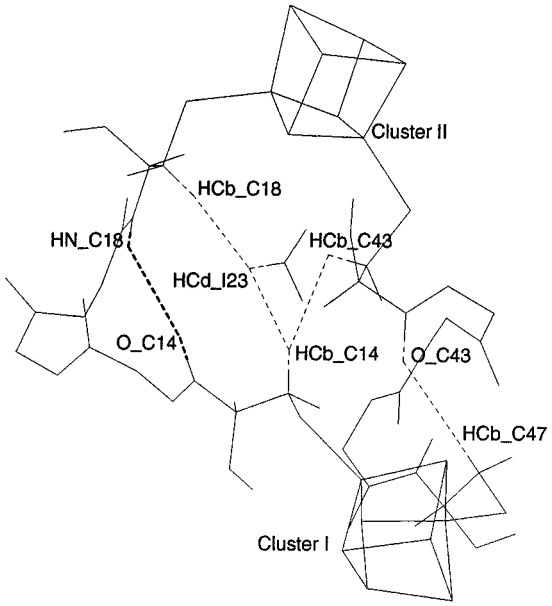

FIGURE 5: Structural details between the two clusters of *C. acidurici* ferredoxin illustrating the most efficient coupling pathways generated by the Greenpath program. Bold and normal dashed lines indicate hydrogen-bond and through-space jumps, respectively.

The influence of side-chain substitutions on the intramolecular ET rate constant has thus to be analyzed through the potential changes they may introduce into the structure between the clusters, i.e., to the conformations of the cysteinyl ligands or of the backbone linking the clusters. The latter segments (residues 14−18 and 43−47) fold as distorted helical turns (Duée et al., 1994). No evidence for strong movements of these parts of the molecule has been found either by ^{1}H NMR in the case of the molecular variants investigated herein (Quinkal et al., 1994; data not shown) or by EPR (Gaillard et al., 1993; data not shown), and their conservation may well be a very important feature for the stability of the molecule. This is not true for the slight conformational changes of the cysteinyl side chains witnessed by chemical shift differences (Gaillard et al., 1993; Table 3). However, the present ET rate constant measurements indicate that the changes in the detailed conformation of the cysteines are not enough to significantly affect the electronic coupling between the clusters (Table 1).

Therefore, the main outcome of the above analysis is that, as long as the relative geometric relationship between the clusters is preserved, the electronic coupling between them is unlikely to vary significantly. However, the components of reorganization energy contribute also to ET rate constants and have to be examined.

Reorganization Energy and Effect of Temperature on the Rate Constant. The results in Figure 3 show that the intramolecular ET rate constant between the clusters of *C. pasteurianum* 2[4Fe-4S] Fd is hardly, if any, dependent on the temperature between 283 and 308 K. However, care must be taken for the interpretation of temperature effects because all three parameters in eq 4, namely, electronic coupling, driving force, and reorganization energy, can be temperature-dependent (Hoffman & Ratner, 1996; Ortega et al., 1996). Moreover, the form of eq 4 might not be adequate

for the description of the system at very low temperatures and, more generally, if the energy of nuclear motions, $h\omega$, associated with ET is large compared to thermal energy, K_BT (Moser et al., 1992; Barbara et al., 1996). It is clear from Figure 3 that the magnitude of the reorganization energy λ associated with long-range ET between the clusters of 2[4Fe-4S] Fds cannot be measured by the temperature dependence of the rate constants. The experimental determination of λ will require the implementation of other methods.

Before this goal is reached, it is worth noticing that the delocalization of electrons over the [4Fe-4S] clusters is expected to result in a small inner reorganization energy λ_i. This suggestion is supported by the limited structural differences occurring between the oxidized and reduced levels of model compounds (Berg et al., 1979; Reynolds et al., 1980). A similar argument concerning a small λ_i due to electron delocalization has been put forward in the numerous cases of ET metalloproteins containing polynuclear clusters, such as, for instance, the dinuclear Cu_A site of cytochrome *c* oxidase (Ramirez et al., 1995) or the octanuclear P-clusters of nitrogenase (Kim & Rees, 1994). However, for many biological redox processes the contribution of λ_o might be the most important one, especially for proteins bearing a high total charge and being highly polar (Moulis & Davasse, 1995), as in the case of 2[4Fe-4S] Fd.

Implications for Related Systems and Conclusions. The good agreement between the experimental data for the intramolecular ET in 2[4Fe-4S] Fd and eq 5 on one hand, and the nearly constant value for several molecular variants of *C. pasteurianum* Fd on the other hand, suggest that electron exchange is mainly controlled by the distance between clusters in this family of redox proteins. One could then propose that the theoretical rate constant for the electron exchange without driving force between F_A and F_B in the PsaC subunit of photosystem I should be of the same order of magnitude. In this case, however, the fact that the system is membrane-bound, the presence of additional subunits and redox cofactors, and the significant driving force (−60 meV, Brettel, 1997) between the two clusters should affect the rate of exchange. In fact, recent studies have addressed this question and values of $3.3 \times 10^4\ s^{-1}$ and $>7 \times 10^5\ s^{-1}$ have been proposed based on flash-induced voltage changes (Sigfridsson et al., 1995) and studies on a covalent complex of PS I and its soluble redox partner ferredoxin (Lelong et al., 1996), respectively. The spread of these values shows the difficulty in resolving the ET process between F_A and F_B in photosystem I. The data presented here suggest that the ET rate constant between the two [4Fe-4S] clusters linked by stretches of three amino acids as found in many biological systems should be around $5 \times 10^6\ s^{-1}$ and relatively independent of the protein considered, when the two clusters have similar reduction potentials. However, this generalization contrasts with the experimental evidence obtained with *Chromatium vinosum* 2[4Fe-4S] Fd, for which a significantly decreased rate constant has been estimated (Huber et al., 1995) despite the very similar geometry of the protein around the clusters (Moulis et al., 1996) when compared with the Fd from *C. acidurici* (Duée et al., 1994). Therefore, the intramolecular electron exchange in 2[4Fe-4S] Fd, in the absence of driving force, might have additional regulating mechanisms, and studies are currently underway in an effort to define the nature of such possible mechanisms.

ACKNOWLEDGMENT

We thank Professor Patrick Bertrand for useful discussions and Dr. Klaus Brettel for sending a preprint of his review and constructive comments on the manuscript. We are also grateful to Dr. J. J. Regan who provided the Greenpath program and to Dr. G. Matthias Ullmann who advised us on its use. Dr. Jacques Meyer is thanked for carefully reading the manuscript.

REFERENCES

Adman, E. T., Sieker, L. C., & Jensen, L. H. (1976) *J. Biol. Chem. 251*, 3801−3806.
Armstrong, F. (1982) in *Advances in Inorganic and Bioinorganic Mechanisms* (Sykes, A. G., Ed.) Vol. 1, pp 65−120, Academic Press, London.
Barbara, P. F., Meyer, T. J., & Ratner, M. A. (1996) *J. Phys. Chem. 100*, 13148−13168.
Benelli, B., Bertini, I., Capozzi, F., & Luchinat, C. (1994) *Gazz. Chim. Ital. 124*, 469−474.
Berg, J. M., Hodgson, K. O., & Holm, R. H. (1979) *J. Am. Chem. Soc. 101*, 4586−4593.
Bertini, I., Briganti, F., Luchinat, C., & Scozzafava, A. (1990) *Inorg. Chem. 29*, 1874−1880.
Bertini, I., Briganti, F., Luchinat, C., Messori, L., Monnanni, R., Scozzafava, A., & Vallini, G. (1992) *Eur. J. Biochem. 204*, 831−839.
Bertini, I., Capozzi, F., Luchinat, C., Piccioli, M., & Vila, A. J. (1994) *J. Am. Chem. Soc. 116*, 651−660.
Brettel, K. (1997) *Biochim. Biophys. Acta 1318*, 322−373.
Capaldi, R. A. (1996) *Nature Struc. Biol. 3*, 570−574.
Carter, C. W., Jr. (1977) in *Iron−Sulfur Proteins* (Lovenberg, W., Ed.) Vol. III, pp 157−204, Academic Press, New York.
Chitnis, P. R. (1996) *Plant Physiol. 111*, 661−669.
Davasse, V., & Moulis, J.-M. (1992) *Biochem. Biophys. Res. Commun. 185*, 341−349.
Davasse, V., Quinkal, I., Gaillard, J., & Moulis, J.-M. (1995) in *Perspectives on Protein Engineering & Complementary Technologies* (Geisow, M. J., & Epton, R., Eds.) pp 152−155, Mayflower Worldwide Limited, Birmingham, U.K.
Duée, E. D., Fanchon, E., Vicat, J., Sieker, L. C., Meyer, J., & Moulis, J.-M. (1994*) J. Mol. Biol. 243*, 683−695.
Einarsdóttir, O. (1995) *Biochim. Biophys. Acta 1229*, 129−147.
Eriksson, A. E., Baase, W. A., Zhang, X.-J., Heinz, D. W., Blaber, M., Baldwin, E. P., & Matthews, B. W. (1992) *Science 255*, 178−183.
Fersht, A. R., & Serrano, L. (1993) *Curr. Opin. Struct. Biol. 3*, 75−83.
Gaillard, J., Moulis, J.-M., Auric, P., & Meyer, J. (1986) *Biochemistry 25*, 464−468.
Gaillard, J., Moulis, J.-M., & Meyer, J. (1987) *Inorg. Chem. 26*, 320−324.
Gaillard, J., Quinkal, I., & Moulis, J.-M. (1993) *Biochemistry 32*, 9881−9887.
Gaillard, J., Zhuang-Jackson, H.-Y., & Moulis, J.-M. (1996) *Eur. J. Biochem. 238*, 346−349.
Gray, H. B., & Winkler, J. R. (1996) *Annu. Rev. Biochem. 65*, 537−561.
Hoffman, B. M., & Ratner, M. A. (1996) *Inorg. Chim. Acta 243*, 233−238.
Huber, J. G., Gaillard, J., & Moulis, J.-M. (1995) *Biochemistry 34*, 194−205.
Johnson, M. K. (1994) in *Encyclopedia of Inorganic Chemistry* (King, R. B., Ed.,) Vol. 4, pp 1896−1915, John Wiley, London.
Karpishin, T. B., Grinstaff, M. W., Komar-Panicucci, S., McLendon, G., & Gray, H. B. (1994) *Structure 2*, 415−422.
Kellis, J. T. J., Nyberg, K., Sali, D., & Fersht, A. R. (1988) *Nature 333*, 784−786.
Kim, J., & Rees, D. C. (1994) *Biochemistry 33*, 389−397.
Krauss, N., Schubert, W.-D., Klukas, O., Fromme, P., Witt, H. T., & Saenger, W. (1996) *Nature Struct. Biol. 3*, 965−973.
Lelong, C., Boekema, E. J., Kruip, J., Bottin, H., Rogner, M., & Sétif, P. (1996) *EMBO J. 15*, 2160−2168.

Lippard, S. J., & Berg, J. M. (1994) *Principles of Bioinorganic Chemistry*, University Science Books, Mill Valley, CA.
Marcus, R. A., & Sutin, N. (1985) *Biochim. Biophys. Acta 811*, 265−322.
Moser, C. C., Keske, J. M., Warncke, K., Farid, R. S., & Dutton, P. L. (1992) *Nature 355*, 796−802.
Moser, C. C., Page, C. C., Farid, R., & Dutton, P. L. (1995) *J. Bioenerg. Biomembr. 27*, 263−274.
Mouesca, J.-M., Rius, G., & Lamotte, B. (1993) *J. Am. Chem. Soc. 115*, 4714−4731.
Moulis, J.-M., & Davasse, V. (1995) *Biochemistry 34*, 16781−16788.
Moulis, J.-M., Davasse, V., & DeJésus, F. (1994) *Biometals 7*, 272−278.
Moulis, J.-M., Sieker, L. C., Wilson, K. S., & Dauter, Z. (1996) *Protein Sci. 5*, 1765−1775.
Navarro, J. A., Cheddar, G., & Tollin, G. (1989) *Biochemistry 28*, 6057−6065.
Nugent, J. H. A. (1996) *Eur. J. Biochem. 237*, 519−531.
Onuchic, J. N., Beratan, D. N., Winkler, J. R., & Gray, H. B. (1992) *Annu. Rev. Biophys. Biomol. Struct. 21*, 349−377.
Ortega, J. M., Mathis, P., Williams, J. C., & Allen, J. P. (1996) *Biochemistry 35*, 3354−3361.
Pace, C. N. (1992) *J. Mol. Biol. 226*, 29−35.
Packer, E. L., Sweeney, W. V., Rabinowitz, J. C., Sternlicht, H., & Shaw, E. (1977*) J. Biol. Chem. 252*, 2245−2253.
Phillips, W. D., & Poe, M. (1973) in *Iron−Sulfur Proteins.* (Lovenberg, W., Ed.) Vol. II, pp 255−285, Academic Press, New York.
Quinkal, I., Davasse, V., Gaillard. J., & Moulis, J.-M. (1994) *Protein Eng. 7*, 681−687.
Quinkal, I., Kyritsis, P., Kohzuma, T., Im, S.-C., Sykes, A. G., & Moulis, J.-M. (1996) *Biochim. Biophys. Acta 1295*, 201−208.
Ramirez, B. E., Malmström, B. G., Winkler, J. R., & Gray, H. B. (1995) *Proc. Natl. Acad. Sci. U.S.A. 92*, 11949−11951.
Regan, J. J., Risser, S. M., Beratan, D. N., & Onuchic, J. N. (1993) *J. Phys. Chem. 97*, 13083−13088.
Regan, J. J., DiBilio, A. J., Langen, R., Skov, L. K., Winkler, J. R., Gray, H. B., & Onuchic, J. N. (1995) *Chem. Biol. 2*, 489−496.
Reynolds, J. G., Coyle, C. L., & Holm, R. H. (1980) *J. Am. Chem. Soc. 102*, 4350−4355.
Robertson, D. E., Farid, R. S., Moser, C. C., Urbauer, J. L., Mulholland, S. E., Pidikiti, R., Lear, J. D., Wand, A. J., DeGrado, W. F., & Dutton, P. L. (1994) *Nature 368*, 425−432.
Sandström, J. (1982) *Dynamic NMR Spectroscopy*, Academic Press, New York.
Sigfridsson, K., Hansson, Ö., & Brzezinski, P. (1995) *Proc. Natl. Acad. Sci. U.S.A. 92*, 3458−3462.
Tsukihara, T., Aoyama, H., Yamashita, E., Tomizaki, T., Yamaguchi, H., Shinzawa-Itoh, K., Nakashima, R., Yaono, R., & Yoshikawa, S. (1996) *Science 272*, 1136−1144.
Walker, J. E. (1992) *Q. Rev. Biophys. 25*, 253−324.
Winkler, J. R., Malmström, B. G., & Gray, H. B. (1995) *Biophys. Chem. 54*, 199−209.

BI970020M